ARTICLE

Nonlocal Chemical Reactivity at Organic–Metal Interfaces

Lan Chen,[†,*] Hui Li,[§] and Andrew Thye Shen Wee[‡,*]

[†]Nanoscience & Nanotechnology Initiative, [‡]Department of Physics, and [§]Department of Chemistry, National University of Singapore, 2 Science Drive 3, 117542, Singapore

ABSTRACT Understanding electron transport at the organic–inorganic interface is crucial for many research fields including surface physics and chemistry. In this article, we report the nonlocal chemical reactivity of one monolayer copper hexadecafluorophthalocyanine (F_{16}CuPc) adsorbed on two different substrates, Ag(111) and Au(111), by injecting hot electrons from a scanning tunneling microscope tip. On the basis of experimental and theoretical results, the nonlocal reactions are proposed to strongly depend on hot-electron transport through molecule–substrate interface states. This observation of nonlocal reactivity increases our understanding of electron transport at organic–metal interfaces.

KEYWORDS: chemical reactions · surface · scanning tunneling microscopy · interface · electron transport

Interfacial charge transport is a topic with relevance in many research fields, including surface physics and chemistry,[1,2] photocatalysis,[3] organic photovoltaics,[4] and molecular electronics.[5] There is much scientific interest to understand the nature and mechanism of charge transport at molecule–metal interfaces.[6,7] In photochemistry on metal surfaces, interfacial electron transport plays a fundamental role in the process of chemical reactions, for example, dissociation reactions, which are induced by hot electrons, that is, electrons photoexcited above the Fermi level of the metal and then transferred to a molecular resonance (*e.g.*, LUMO).[2,6,8] It would be interesting if we could measure the electron transport process *via* direct analysis of electron-induced reactions at the molecule–metal interface.

In the past decade, scanning tunneling microscopy (STM) has been developed from an imaging instrument to a powerful technique to directly investigate chemical reactivity on surfaces.[9,10] Unlike chemical reactions in surface photochemistry, electrons from an STM tip are directly injected into molecular states. The tunneling electrons from an STM tip are spatially localized at the atomic scale and have a large current density of ~1 MA/cm^2. The ultrahigh current density in STM allows electron-induced chemical reactions to be observed. Most STM studies have focused on single-molecular chemistry,[9,10] where the molecule investigated is directly located at the point of electron injection. Nonlocal reactivity of molecules has been reported in several cases and was thought to be caused by the electric field in the tunneling junction,[11] hot electrons propagating in the metal surface,[12] organic thin film,[13] and self-assembled molecular chains.[14]

Here we demonstrate that hot electrons injected from an STM tip can cause different nonlocal chemical reactions in one monolayer of copper hexadecafluorophthalocyanine (F_{16}CuPc) adsorbed on two different metal surfaces, Ag(111) and Au(111). On the basis of experimental results and density functional theory (DFT) calculations, we propose that the nonlocal reactions were mainly induced by hot-electron transport in the interface states formed between the adsorbed molecules and metal substrate. Such electron-induced chemical reactivity at the molecular scale offers an alternative method of investigating the electron transport process at molecule–metal interfaces.

RESULTS AND DISCUSSION

F_{16}CuPc molecules (the molecular structure is shown in the inset of Figure 1a) adsorbed on the Ag(111) and Au(111) appear as four-leaf-like protrusions with four-fold symmetry, and each leaf corresponds to one F-substituted peripheral benzene ring, as shown in Figure 1a,b, respectively. F_{16}CuPc molecules assemble along the [1−10] direction of Ag(111), forming well-ordered molecular rows with two different in-plane orientations. The lattice of molecular rows is commensurate with the substrate,

See the accompanying Perspective by MacLeod *et al.* on p 3347.

*Address correspondence to nnicl@nus.edu.sg (L. Chen), phyweets@nus.edu.sg (A.T.S. Wee).

Received for review July 16, 2009 and accepted October 27, 2009.

Published online October 30, 2009. 10.1021/nn900811t CCC: $40.75

and the two kinds of molecular rows are mirrored structures with small lateral displacement.[15] Similarly, F_{16}CuPc molecules on Au(111) also self-assemble into commensurable molecular rows with two different in-plane orientations, and there is also glide-mirror symmetry for the two kinds of rows. The structure models of F_{16}CuPc adsorbed on both surfaces are shown in Figure 1e,f.

After applying a pulse on the target molecule on Ag(111), we observed that one of the four ligands had disappeared (Figure 1c and Figure 2b). Such a chemical reaction was not limited to the molecule under the STM tip. As shown in Figure 1c (pulsed at −3.0 V tip bias, 3.5 nA, 50 ms), the reactions occurred on five molecules at different distances from the STM tip, too. This nonlocal chemical reaction can be observed as far as 12 nm from the STM tip in some cases (not shown here). Similar nonlocal behavior was also observed for molecules on Au(111), shown in Figure 1d (pulsed at −3.2 V, 10 nA, 0.5 s). The magnified STM image (Figure 2c) showed that one ligand of the reacted molecule is also shortened by the pulse. We statistically analyzed the reaction rate (in our experiments, the reaction rate is defined as the total number of reaction events found after of a pulse with a unit time applied) as a function of pulse bias, as shown in Figure 3.

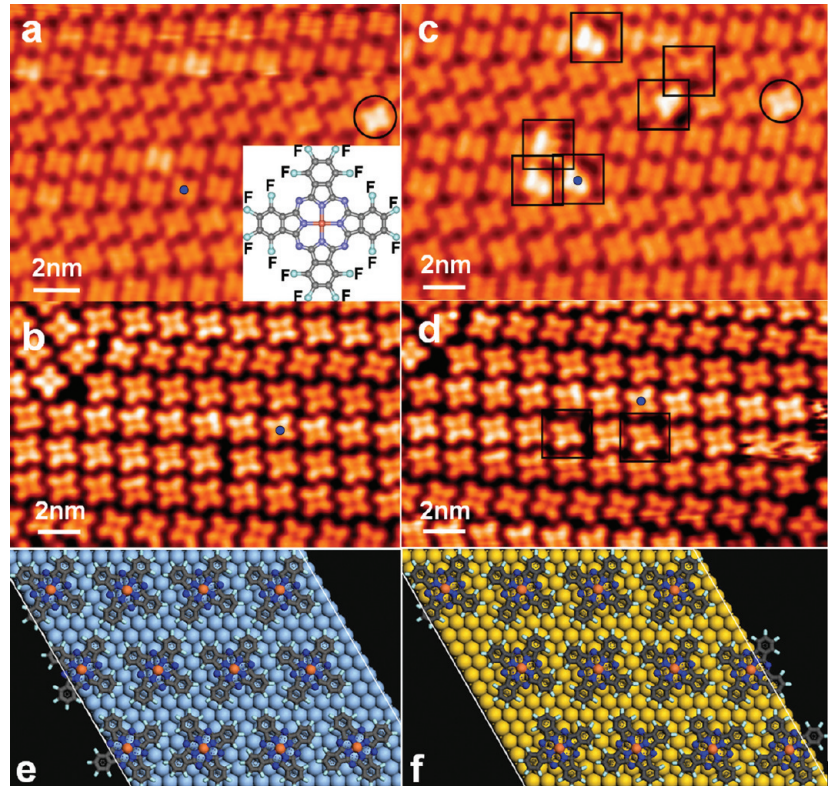

Figure 1. (a,b) STM images of F_{16}CuPc molecules adsorbed on Ag(111) surface and Au(111) surface before pulsing, respectively. (c,d) STM images of F_{16}CuPc molecules on Ag(111) and Au(111) after a pulse at −3.0 and −3.2 V on top of a molecule, respectively. The blue dot, rectangles, and circles represent pulsing position, reacted molecules, and bright molecules not induced by pulsing, respectively. (e,f) Proposed structure models of F_{16}CuPc on Ag(111) and Au(111), respectively.

We determined the energy onset for this nonlocal chemical reaction in F_{16}CuPc molecules on Ag(111) to be ∼−1.9 V (tip bias) (Figure 3a). For Au(111), the corresponding energy onset is ∼−2.4 V (Figure 3b). We repeated the experiments at positive tip bias up to 4.0 V, but no reaction events were observed. The reactions only occurred at negative tip bias whereby electrons were injected into molecules from the tip during the applied pulse, indicating the chemical reactions were caused by electrons and not holes. The relatively high energy suggests that the reaction proceeds *via* electronic excitations of the molecules rather than vibrational excitations in the electronic ground states.[9]

We investigated the single-molecule reaction rate (only counting local reacted molecules) as a function of the tunneling current. If the reaction is induced by tunneling electrons, the reaction rate R_0, the current I_0, and the reaction order n should obey the relation $R_0 = I_0^N$ (ref 10). The results obtained for molecules on Ag(111) and Au(111) are shown in Figure 4a,b. The lines in the graph correspond to the results of the linear fitting, where the slopes are determined to be 4.2 ± 0.2 for Ag(111) and 1.9 ± 0.2 for Au(111). This rules out the possibility of reaction induced by electric field because the reaction rate is very sensitive to variation of tunneling current. Thus, we deduce that the reaction order is ∼4 (∼2) for Ag (Au) and interpret the single-molecule reaction as a four-electron (two-electron) process for molecules on Ag(111) (Au(111)). The quantum yield for the single-molecule re-

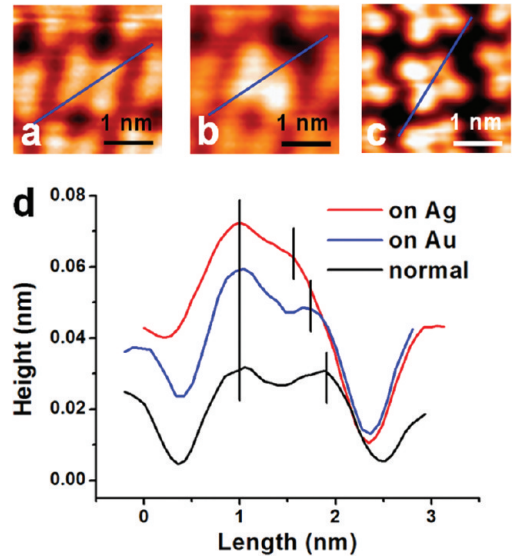

Figure 2. (a) Magnified STM image of the single unreacted F_{16}CuPc molecule on Ag(111). (b,c) STM images of reacted molecules on Ag(111) and Au(111), respectively. (d) Line profiles along the blue lines in (a)−(c).

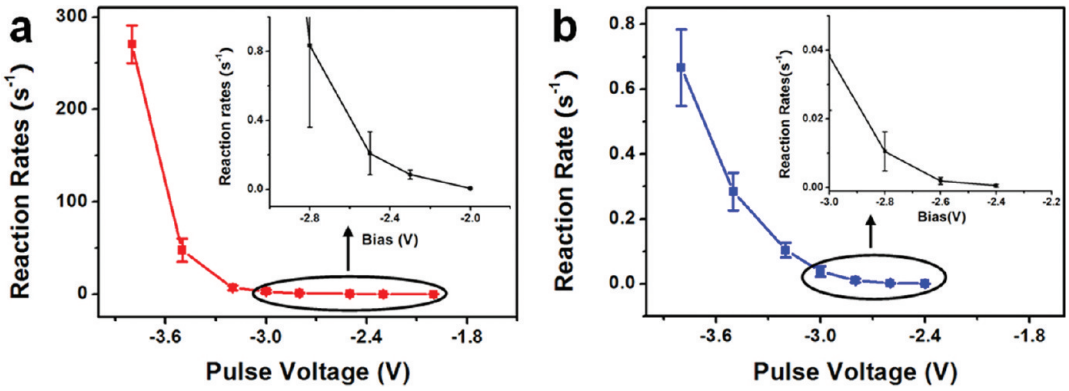

Figure 3. (a,b) Event rates of the nonlocal reactions as a function of excitation energy for molecules on Ag(111) and Au(111), respectively. The parts of curves at lower energy are magnified and shown in the insets. The excitation pulse (I = 5 nA) is applied at a molecule near the center of the field of view, and the reaction events were counted in the surrounding area of 400 nm^2.

action on Ag(111) is about 10^{-10} events per electron, 2 orders of magnitude higher than that on Au(111).

The changes observed in the molecules in the STM images may be the consequence of electron-induced molecular conformational change[16] or dissociation.[17] Unlike metallotetraphenylporphyrin, which has two conformations on the metal surface and can be switched by a voltage pulse from the STM tip,[16] F_{16}CuPc is a planar, conjugated, and rigid molecule.[18] Only one lying-down configuration with its molecular π-plane parallel to the surface can be found when adsorbed on Ag(111) and Au(111).[15] Electron-induced molecular conformational change is ruled out. The line profiles across the reacted molecules (Figure 2d) indicate that one ligand has been shortened. This observation is very similar to the reported dehydrogenation reaction induced by STM on the benzene ring of cobalt phthalocyanine (CoPc).[17] The ligand with the dehydrogenated benzene ring also appeared shortened in the STM image. We believe the similar C−F bond dissociation can also result in the observed shorter ligand. Furthermore, electron-induced dissociation of the C−H bond in benzene,[19] C−Cl bond in chlorobenzene,[20] and C−I bond in iodobenzene[21] on a metal surface has been previously reported. The mechanism is known as dissociative electron attachment (DEA),[22] in which electrons with specific energies can be captured into the antibonding π^* orbitals of molecule, and then transferred into the σ^* orbital, causing bond breaking and generating ions. Therefore, we conclude that our observed chemical reaction results from the defluorination of the benzene ring (C−F bond dissociation) in F_{16}CuPc. If one electron is needed to break one C−F bond in the DEA mechanism, there are in total four (two) C−F bond dissociations in the reacted ligand of F_{16}CuPc on the Ag(111) (Au(111)) surface. The different lengths of the defluorinated ligands of the reacted molecules on Au(111) and Ag(111) (Figure 2d) are consistent with the different number of C−F bond dissociations for reacted molecules on different surfaces.

The identical shapes of all reacted molecules in the STM images indicate that similar defluorination reactions had

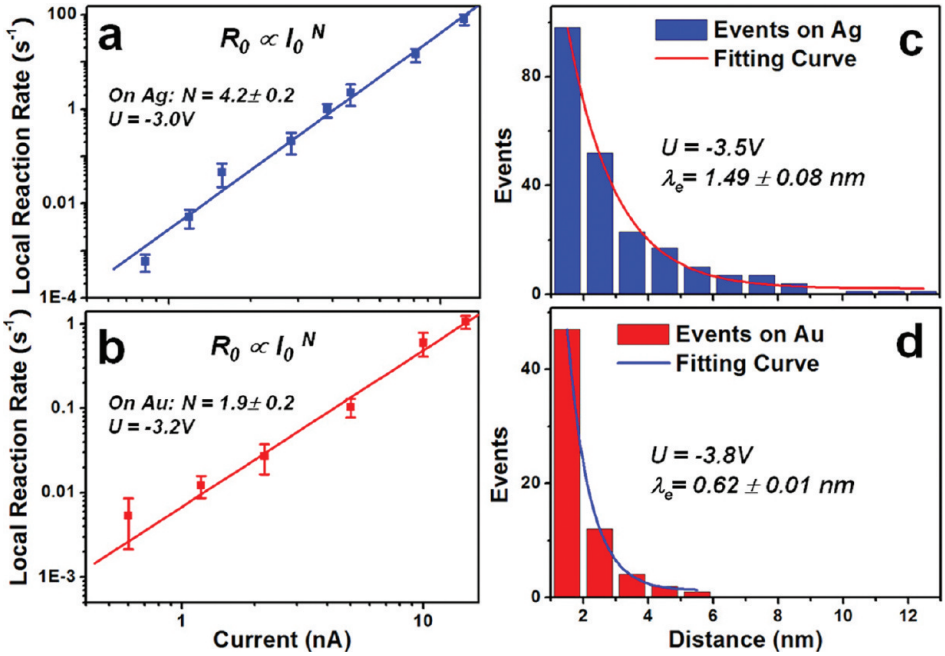

Figure 4. (a,b) Kinetics of single-molecule chemical reactions locally under STM tip on Ag(111) and Au(111) obtained from statistical analysis of 1000 single-molecule reactions. Solid lines are linear fits to the data of the reaction rate as a function of tunneling current in the log−log coordinates. (c,d) Spatial attenuation of events of nonlocal reactions obtained from statistical analysis of several hundred molecules on Ag(111) and Au(111). Solid lines are exponential decay fits to the data.

occurred, caused by hot-electron transport into π^* molecular orbitals. To explain the nonlocal reactions, the mechanism of lateral hot-electron propagation is proposed. The hot-electron origin of nonlocal reactions is confirmed from the statistical analysis of radial distribution of reaction events using the equation $P_r \propto (I_0 f(r))^N$ (ref 12). Here, P_r is the number of reacted molecules, and $f(r)$ is the attenuation function. This equation connects the nonlocal reactions at radius r to the hot-electron current (I_r). As seen in Figure 4c,d, the reaction events on Ag(111) and Au(111) obey a lateral exponential decay function, $P_r \propto e^{-r/\lambda_e}$. The decay length λ_e is about 1.5 nm for reactions on Ag(111) and 0.6 nm for Au(111). The nonlocal chemical reactions could also be induced by electrons from a blunt STM tip. To rule out this possibility, we repeated this experiment using several different tips and obtained similar values of decay lengths (one example shown in Figure S1 in the Supporting Information). These decay lengths show little dependence on the STM tip. On the basis of the attenuation function, $f(r) \propto e^{-r/N\lambda_e}$, we obtain the current decay length, $\lambda_I = N\lambda_e = 6$ nm for Ag(111) and 1.2 nm for Au(111), Therefore, λ_I can represent the characteristic lateral attenuation of hot-electron current.

We have observed novel nonlocal chemical reactivity of one monolayer of F_{16}CuPc adsorbed on different metal surfaces, Ag(111) and Au(111), induced by electron injection from STM tip, and presented significant differences in reaction behavior, including number of C−F bond dissociations, quantum yield, and lateral decay length of hot current. The reaction behavior is attributed to the process of hot-electron transport and propagation, which we propose occurs *via* molecule/metal interface states. The electron propagation through the molecular layer itself is another alternative mechanism.[23] However, as F_{16}CuPc adopts a lying-down configuration with its molecular π-plane parallel to the surface, the coupling of two adjacent molecules should be very small due to the negligible overlap of π orbitals in the $x-y$ plane between neighboring molecules with a center-to-center distance as large as 1.5 nm. On the other hand, if the nonlocal chemical reactions are induced by electron propagation through the molecular layer, the decay lengths for different surfaces must be identical, which is contrary to our experimental results. Hence, this alternative mechanism is ruled out.

DFT calculations were carried out to identify the molecule−metal interface states involved. The optimized F_{16}CuPc adsorption geometry from DFT calculations on Ag(111) and Au(111) shown in Figure 5a,b suggests a lying-down but significantly distorted configuration. The outer fluorine atoms are located 0.2 Å (0.09 Å) further away from the Ag(111) (Au(111)) surface, in agreement with previous experiments.[24] Larger deviation of F atoms from the molecular plane may weaken C−F bonds in F_{16}CuPc on Ag(111) relative to those on Au(111). This might be one reason for the different number of C−F bond breaking observed for F_{16}CuPc on Ag(111) and Au(111).

The calculated projected density of states (PDOS) of F_{16}CuPc/Ag(111) and F_{16}CuPc/Au(111) shown in Figure 5c,d gives the different distributions of molecular orbitals, reflecting the different molecule−metal interactions. Analysis of the spatial distributions of orbital charge densities of all peaks in Figure 5c reveals that the peak around 1.8 eV above the Fermi level consists primarily of the π^* orbital of benzene rings and p and d orbitals of Ag metal atoms, which corresponds to the state trapping hot electrons. Large overlapping between carbon atomic orbitals in the benzene rings and Ag atoms is observed (Figure 5e,f), forming a "bridge" between the molecule and metal surface. Neighboring molecules are connected to each other through these delocalized interface states. A similar state is found at around 2.3 eV above the Fermi level for the F_{16}CuPc/Au(111) system. The different energy positions of the states accord well with the experimental data, explaining the different energy onset for molecules on Ag(111) (−1.9 V) and Au(111) (−2.4 V).

We propose a possible model to explain how the nonlocal reaction is induced by hot-electron transport at the molecule/metal interface, as shown in the electron dispersion schemes in F_{16}CuPc/Ag(111) and F_{16}CuPc/Au(111) (Figure 6). First (step I), the hot electron is injected into the π^* orbital of the benzene ring of F_{16}CuPc from the STM tip to form an excited anion state. In general, the anion state on metal surfaces has a very short lifetime (up to a few tens of femtoseconds).[25,26] Nevertheless, a small fraction of F_{16}CuPc anions could react before electron detachment, whereby the electrons in π^* orbitals transfer into σ^* orbitals of C−F bonds to break the bonds and generate F^- ions. In our experiment, the average interval time between two tunneling electrons is larger than 10 ps (tunneling current ≤10 nA), which is about 3 orders of magnitude larger than the lifetime of the anion state. We deduce that dissociation of four (two) C−F bonds of the molecule on Ag(111) (Au(111)) does not occur simultaneously but successively.

On metal surfaces, however, the most efficient decay process of this anion state is a one-electron energy-conserving electron transfer process in which the hot electron is resonantly transferred into the continuum of metal states (resonant electron transfer (RET process)).[26] The large overlapping of π^* orbitals of F_{16}CuPc and p_z orbitals of the underlying metal atoms forms a delocalized interface state, promoting the RET process without involving a dissociation reaction (step II). From the spatial charge density distribution (Figure 5e−g), we find larger overlapping between carbon atomic orbitals in the benzene rings of F_{16}CuPc and Au atoms (Figure 5g) than that for F_{16}CuPc/Ag(111). The stronger

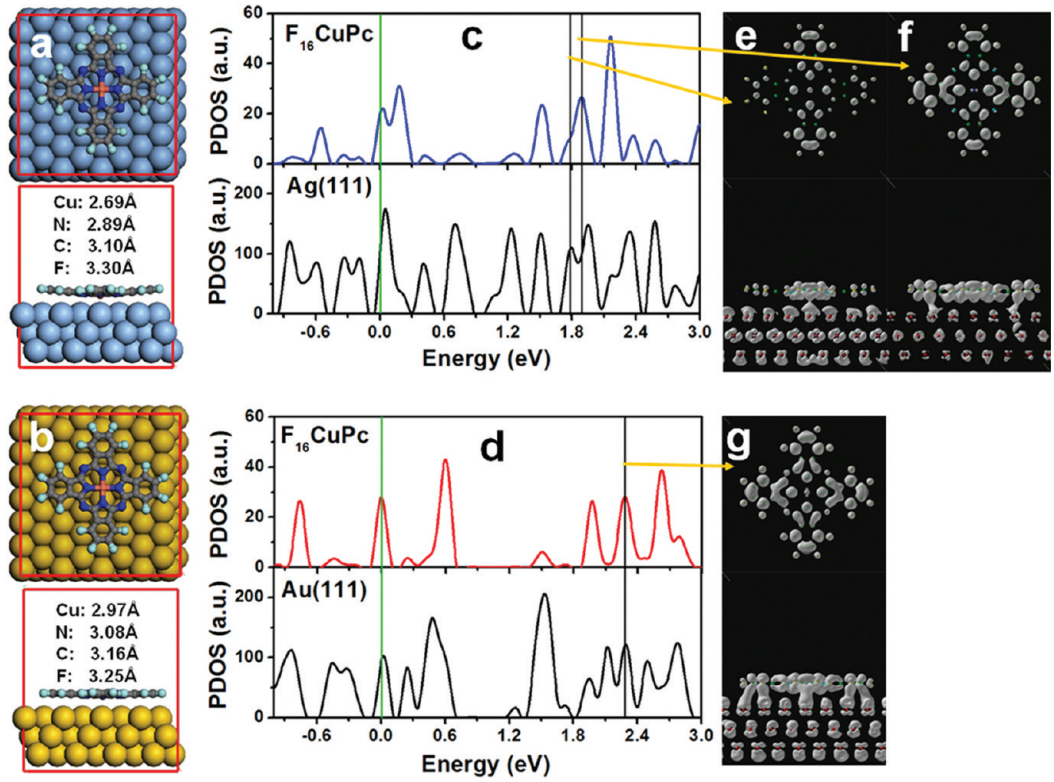

Figure 5. (a,b) Top (upper) and side (lower) view of the optimized computational model for the F_{16}CuPc/Ag(111) and F_{16}CuPc/Au(111) adsorption system, respectively. The vertical distances of various atoms of F_{16}CuPc from surface are indicated. (c,d) PDOS of F_{16}CuPc molecule (upper) and surface atoms (lower) in F_{16}CuPc/Ag(111) and F_{16}CuPc/Au(111) systems, respectively. The green lines indicate the position of Fermi energy. The peaks marked by black lines correspond to hybrid orbitals of molecule and surface metal atoms involved in the chemical reactions. (e−g) Top (upper) and side (lower) view of the spatial distributions of charge density around the energy regions marked by black lines in (c) and (d).

overlapping for F_{16}CuPc/Au shortens the lifetime of the anion state and lowers the probability of chemical reactions compared with F_{16}CuPc/Ag. This may explain why the quantum reaction yield on Au(111) is much smaller than that on Ag(111).

The adsorbate-induced delocalized interface state (1.8 and 2.3 eV above the Fermi level) lies within the Γ-centered projected bulk band gap of Ag(111)[27] and Au(111),[28] causing electron transfer from surface to the bulk to be less likely in the direction normal to the surface. Thus, the mixing of molecular orbitals with metal surface states is the main channel facilitating the propagation of hot electrons with horizontal momentum (step III). In fact, the Ag(111) orbital at 1.8 eV above the Fermi energy comprises p_x and p_y orbitals of Ag, while the Au(111) orbital at 2.4 eV comprises d_{xz} and d_{yz} orbitals of Au. The larger orbital spatial extension in the *xy* plane of Ag means that the delocalization of the interface state of F_{16}CuPc/Ag(111) is larger than that of F_{16}CuPc/Au(111). This may explain the different charge transport efficiencies and current lateral decay lengths λ_l in the two surfaces. Electrons propagating in a metal surface can back-transfer into the π* orbitals of another molecule through this reversible "bridge" formed between molecule and substrate (step IV), leading to another defluorination reaction.

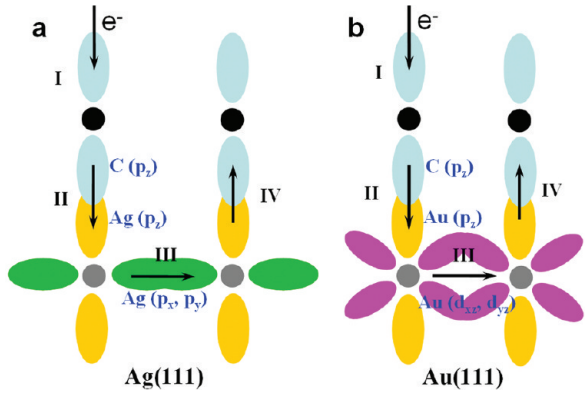

Figure 6. Schematic cartoons illustrating the electron transport process. Electron capture in π* orbitals of molecules (step I), transfer from molecule to surface metal atoms (II), propagation in hybridized states of metal atoms (III), then back capture in π* orbitals of another molecule (IV) on (a) Ag(111) and (b) Au(111). Black and gray solid circles represent C atoms of molecules and metal atoms at the surface.

CONCLUSION

In conclusion, we have observed nonlocal electron-induced chemical reactivity at two different organic−metal interfaces by STM and propose a model to explain how the reaction is induced by molecular−metal interactions. This study demonstrates a direct method to explore interfacial reaction dynam-

ics by STM and links the fields of STM-induced chemistry to photochemistry of adsorbed molecules. This work also provides an approach to characterize and understand the nature of charge transport through interface states. Further work including experiments and theoretical calculations is still needed to study the detailed dynamic process of hot-electron transport at the organic−metal interface.

METHODS AND THEORETICAL CALCULATIONS

The experiments were carried out in a low-temperature STM (Omicron Nano Technology GmbH) interfaced with a Nanonis controller (Nanonis, Switzerland) in an ultrahigh vacuum chamber ($<5 \times 10-11$ Torr).[29] The Ag(111) and Au(111) surfaces were prepared using Ar^+ sputtering−annealing cycles. One monolayer of $F_{16}CuPc$ molecules was deposited from Knudsen cells (MBE-Komponenten, Germany) at 380 °C on substrates held at room temperature. The sample was subsequently transferred to the STM chamber and cooled to liquid nitrogen temperature (77 K) for STM experiments. All STM images were obtained using chemical-etched tungsten tips (cleaned by circular Ar^+ sputtering at 500−800 V for about 5−10 min). We initially used a constant current mode with relative low bias voltage and tunneling current (typically voltage $|V| < 1.5$ V and current $|I| < 0.2$ nA) to image the molecules. Subsequently, the STM tip was positioned over the center of a target molecule, the feedback loop was turned off, and a pulse with defined voltage and current was applied on the molecule. The same area was then scanned again with the same scanning parameters to image the reaction products. Figure 1 shows an example how reaction events were collected and counted.

In DFT calculations, the computational model contained one $F_{16}CuPc$ molecule lying on $7 \times 8 \times 3$ layers of Ag/Au atoms, and the vertical extension was chosen to be 23.6 Å. The calculations were within the framework of the local density approximation (LDA)[30] using the ultrasoft pseudopotential (USPP)[31] basis sets with the Vienna *ab initio* simulation package (VASP).[32] The corresponding plane wave cutoff was at 424.3 eV, and only the Γ point was considered in the Brilliouin zone due to the large unit cell.

Acknowledgment. The authors acknowledge funding support from A*STAR grant number R-398-000-036-305, and the Singapore Millenium Foundation (SMF) for a Fellowship to L.C.

Supporting Information Available: Spatial distribution of nonlocal reactions in Ag(111) and Au(111) surfaces induced by another STM tip. This material is available free of charge *via* the Internet at http://pubs.acs.org.

REFERENCES AND NOTES

1. Zhu, X. Y. Surface Photochemistry. *Annu. Rev. Phys. Chem.* **1994**, *45*, 113–144.
2. Lindstrom, C. D.; Zhu, X. Y. Photoinduced Electron Transfer at Molecule−Metal Interface. *Chem. Rev.* **2006**, *106*, 4281–4300.
3. Linsebigler, A. L.; Lu, G. Q.; Yates, J. T., Jr. Photocatalysis on TiO_2 Surfaces—Principles, Mechnisms, and Selected Results. *Chem. Rev.* **1995**, *95*, 735–758.
4. Ho, P. K. H.; Kim, J. S.; Burroughes, J. H.; Becker, H.; Li, S. F. Y.; Brown, T. M.; Cacialli, F.; Friend, R. H. Molecular-Scale Interface Engineering for Polymer Lighting-Emitting Diodes. *Nature* **2000**, *404*, 481–484.
5. Nitzan, A.; Ratner, M. A. Electron Transport in Molecular Wire Junctions. *Science* **2003**, *300*, 1384–1389.
6. Zhu, X. Y. Electronic Structure and Electron Dynamics at Molecule−Metal Interfaces: Implications for Molecule-Based Electronics. *Surf. Sci. Rep.* **2004**, *56*, 1–83.
7. Wang, L.; Chen, W.; Wee, A. T. S. Charge Transfer Across the Molecule/Metal Interface Using the Core Hole Clock Technique. *Surf. Sci. Rep.* **2008**, *63*, 465–486.
8. Dixon-Warren, J.; Jensen, E. T.; Polanyi, J. C. Direct Evidence for Charge-Transfer Photodissociation at a Metal Surface: CCl_4/Ag(111). *Phys. Rev. Lett.* **1991**, *67*, 2395–2398.
9. Ho, W. Single-Molecule Chemistry. *J. Chem. Phys.* **2002**, *117*, 11033–11061.
10. Komeda, T. Chemical Identification and Manipulation of Molecules by Vibrational Excitation *via* Tunneling Process with Scanning Tunneling Microscopy. *Prog. Surf. Sci.* **2005**, *78*, 41–85.
11. Alemani, M.; Peters, M. V.; Hecht, S.; Rieder, K.-H.; Moresco, F.; Grill, L. Electric Field-Induced Isomerization of Azobenzene by STM. *J. Am. Chem. Soc.* **2006**, *128*, 14446–14447.
12. Maksymovych, P.; Dougherty, D. B.; Zhu, X. Y.; Yates, J. T. Nonlocal Dissociative Chemistry of Adsorbed Molecules Induced by Localized Electron Injection into Metal Surfaces. *Phys. Rev. Lett.* **2007**, *99*, 016101.
13. Nouchi, R.; Masunari, K.; Ohta, T.; Kubozono, Y.; Iwasa, Y. Ring of C_{60} Polymers Formed by Electron or Hole Injection from a Scanning Tunneling Microscope Tip. *Phys. Rev. Lett.* **2006**, *97*, 196101.
14. Maksymovych, P.; Sorescu, D. C.; Jordan, K. D.; Yates, J. T. Collective Reactive of Molecular Chains Self-Assembled on a Surface. *Science* **2008**, *322*, 1664–1667.
15. Huang, H.; Chen, W.; Wee, A. T. S. Low-Temperature Scanning Tunneling Microscopy Investigation of Epitaxial Growth of $F_{16}CuPc$ Thin Film on Ag(111). *J. Phys. Chem. C* **2008**, *112*, 14913–14918.
16. Lancu, V.; Deshpande, A.; Hla, S.-W. Manipulating Kondo Temperature *via* Single Molecule Switching. *Nano Lett.* **2006**, *6*, 820–823.
17. Zhao, A. D.; Li, Q. X.; Chen, L.; Xiang, H. J.; Wang, W. H.; Pan, S.; Wang, B.; Xiao, X. D.; Yang, J. L.; Hou, J. G.; *et al.* Controlling the Kondo Effect of an Adsorbed Magnetic Ion through Its Chemical Bonding. *Science* **2005**, *309*, 1542–1544.
18. Ghosh, A.; Gassman, P. G.; Almlof, J. Substituent Effects in Porphyrazines and Phthalocyanines. *J. Am. Chem. Soc.* **1994**, *116*, 1932–1940.
19. Komeda, T.; Kim, Y.; Fujita, Y.; Sainoo, Y.; Kawai, M. Local Chemical Reaction of Benzene on Cu(110) *via* STM-Induced Excitation. *J. Chem. Phys.* **2005**, *120*, 5347–5352.
20. Sloan, P. A.; Palmer, R. E. Two-Electron Dissociation of Single Molecules by Atomic Manipulation at Room Temperature. *Nature* **2005**, *434*, 367–371.
21. Hla, S. W.; Bartels, L.; Meyer, G.; Rieder, K. H. Inducing All Steps of a Chemical Reaction with the Scanning Tunneling Microscope Tip: Towards Single Molecule Engineering. *Phys. Rev. Lett.* **2000**, *85*, 2777–2780.
22. Palmer, R. E. Electron-Molecule Dynamics at Surfaces. *Prog. Surf. Sci.* **1992**, *41*, 51–108.
23. Liljeroth, P.; Repp, J.; Meyer, G. Current-Induced Hydrogen Tautomerization and Conductance Switching of Naphthalocyanine Molecules. *Science* **2007**, *317*, 1203–1206.
24. Gerlach, A.; Schreiber, F.; Sellner, S.; Dosch, H.; Vartanyants, I. A.; Cowie, B. C. C.; Lee, T. L.; Zegenhagen, J. Adsorption-Induced Distortion of $F_{16}CuPc$ on Cu(111) and Ag(111): An X-ray Standing Wave Study. *Phys. Rev. B* **2005**, *71*, 205425.
25. Bartels, L.; Meyer, G.; Rieder, K. H.; Velic, D.; Knoesel, E.; Hotzel, A.; Wolf, M.; Ertl, G. Dynamics of Electron-Induced Manipulation of Individual CO Molecules on Cu(111). *Phys. Rev. Lett.* **1998**, *80*, 2004–2007.
26. Chulkov, E. V.; Borisov, A. G.; Gauyacq, J. P.; Sanchez-Portal, D.; Silkin, V. M.; Zhukov, V. P.; Echenique, P. M. Electronic Excitations in Metals and at Metal surfaces. *Chem. Rev.* **2006**, *106*, 4160–4206.
27. Hulbert, S. L.; Johnson, P. D.; Stoffel, N. G.; Smith, N. V. Unoccupied Bulk and Surface States on Ag(111) Studied by Inverse Photoemission. *Phys. Rev. B* **1985**, *32*, 3451–3455.

28. Woodruff, D. P.; Royer, W. A.; Smith, N. V. Empty Surface States, Image States, and Band Edge on Au(111). *Phys. Rev. B* **1986**, *34*, 764–767.
29. Chen, L.; Chen, W.; Huang, H.; Zhang, H. L.; Yuhara, J.; Wee, A. T. S. Tunable Arrays of C_{60} Molecular Chains. *Adv. Mater.* **2008**, *20*, 484–488.
30. Perdew, J. P.; Zunger, A. Self-interaction Correction to Density-Function Approximations for Many-Electron Systems. *Phys. Rev. B* **1981**, *23*, 5048–5079.
31. Kresse, G.; Hafner, J. Norm-Conserving and Ultrasoft Pseudopotentials for First-Law and Transition-Elements. *J. Phys.: Condens. Matter* **1994**, *6*, 8245–8257.
32. Kresse, G.; Furthmüller, J. Efficient Iterative Schemes for *Ab Initio* Total-Energy Calculations Using a Plane-Wave Basis Set. *Phys. Rev. B* **1996**, *54*, 11169–11186.